Supplementary Information

Shape Fixing via Salt Recrystallization: A Morphology-Controlled Approach To Convert Nanostructured Polymer to Carbon Nanomaterial as a Highly Active Catalyst for Oxygen Reduction Reaction

Wei Ding, Li Li, Kun Xiong, Yao Wang, Wei Li, Yao Nie, Siguo Chen, Xueqiang Qi, Zidong Wei *

Chongqing Key Laboratory of Chemical Process for Clean Energy and Resource Utilization, School of Chemistry and Chemical Engineering, Chongqing University, Shazhengjie 174, Chongqing, 400044, China

*zdwei@cqu.edu.cn

Experimental Section

Characterization

Low-resolution transmission electron microscopy (TEM) was carried out on a FEI Tecnai G2 20S-TWIN instrument operating at 120 kV. High-resolution transmission electron microscopy (HRTEM) was carried out on a Zeiss LIBRA 200 FETEM instrument operating at 200 kV. XPS was acquired using a Kratos XSAM800 spectrometer equipped with a monochromatic Al X-ray source (Al KR, 1.4866 keV). High-resolution elemental analysis was performed on the N 1s (390–410 eV) and O 1s (545–525 eV) regions with a pass energy of 20 eV, a step of 0.05 eV, and an 800 ms dwell time. Each spectrum was constructed from an average of two scans. The pressure in the XPS analysis chamber was maintained at 10^{-7} Pa or lower during collection. In the data analysis, the binding energy (BE) of the core level C 1s peak was set at 284.5 eV to compensate for surface-charging effects. The Shirley background was subtracted, and the satellite peaks were removed for all element peaks before curve fitting. The experimental spectra were fitted into a Gaussian line shape. The surface elemental compositions were determined by the ratios of peak areas that had been corrected with empirical sensitivity factors.

Electrochemical measurements

All electrochemical experiments were performed in a standard three-electrode cell at room temperature (298 K). The cell consisted of a glassy carbon working electrode (GC electrode, 3 mm in diameter, PINE: AFE3T050GC), an Ag/AgCl (3M KCl) reference electrode, and a platinum foil counter electrode. All potentials in this study, however, are given relative to a reversible hydrogen electrode (RHE). The working electrodes were prepared by applying catalyst ink onto glassy carbon (GC) disk electrodes. In brief, the electrocatalyst was dispersed in ethanol and ultrasonicated for 15 minutes to form a uniform catalyst ink. A total of 3 μL of well-dispersed catalyst ink was applied onto a prepolished GC disk. After drying at room temperature, a drop of 0.05 wt% Nafion solution was applied onto the surface of the catalyst layer to form a thin protective film. The prepared electrodes were dried overnight at room temperature before the electrochemical tests. All of the electrodes were pretreated by cycling the potential between 0.05 and 1.1 V at a sweep rate of 50 mVs^{-1} for 50 cycles in order to remove any surface contamination prior to ORR activity testing.

RDE measurements were conducted at rotation speeds from 100 to 2500 rpm using an Autolab Model. RDE measurements were conducted in O_2-saturated 0.5 M H_2SO_4 solution at 10mV/s scan rate. The electron transfer number (n) and kinetic current density (j_k) were analyzed on the basis of Koutecky–Levich equations shown in Equstions. (1)-(3).

$$\frac{1}{j} = \frac{1}{j_d} + \frac{1}{j_k} \tag{1}$$

$$j_d = 0.6nFCD^{2/3}\nu^{-1/6}\omega^{-1/2} = B\omega^{-1/2} \tag{2}$$

$$\frac{1}{j} = \frac{1}{B\omega^{-1/2}} + \frac{1}{j_k} \tag{3}$$

The constant B is $0.6nFCD^{2/3}v^{-1/6}$, where n is the number of electrons in the ORR, C is the bulk concentration of oxygen (1.13×10^{-6}molcm^{-3}), D is the diffusion coefficient of oxygen in the sulfuric acid solution (1.8×10^{-5} cm^{2}s^{-1}) and is the kinematic viscosity of the sulfuric acid (1.0×10^{-2} cm^{2}s^{-1}).

RRDE experiments were conducted using 0.1M $HClO_4$ to preventPt/C performance loss caused by bisulfate adsorption. In the RRDE experiments, the ring potential was set to 1.2 V. Before the experiments, the Pt catalyst in the ring was activated throughpotential cycling in 0.5 M $HClO_4$ from 0 to 1.4 V at a scan rate of 50 mV s^{-1} for 10 minutes. RDE/RRDE rotating speed: 900 rpm; non-Pt catalyst loading: 0.6 mg/cm^2; Pt/C (40%) loading: 50 μgPtcm^{-2}; scan rate: 10 mVs^{-1}. The background current measured in N_2-saturated 0.1 M $HClO_4$ has been subtracted from each LSV curve.The four-electron selectivity of catalysts was evaluated based on the H_2O_2 yield, which was calculated from the following equation (4):

$$H_2O_2 = 200\frac{\mathrm{i_{ring}}/\mathrm{N}}{\mathrm{i_{ring}}/\mathrm{N} + \mathrm{i_{disk}}} \tag{4}$$

Wherei_{disk} and i_{ring} is the disk and ring currents, respectively, and N is the ring collection efficiency. The ring collection efficiency was independently determined using 10 mM $K_3[Fe(CN)_6]$ in 0.1 M KNO_3 solution and a NG catalyst on a carbon disk at a “typical” loading of 0.6 mgcm^{-2}. The measured N value was 36.7%, which is similar to the RDE manufacturer’s value of 37%.

RDE cycling stability tests of the catalysts were performed in N_2-saturated 0.5 M H_2SO_4 in the potential range of 0 to 1.2 V vs. RHE at room temperature (O_2 cycling).

Fuel cell testing. Catalysts were tested in the fuel cell cathode to evaluate their activity. The catalyst “ink” was prepared by ultrasonically mixing the catalyst powder with 5wt % Nafion solution (DuPont), carbon powder (Vulcan XC-72, Cabot Corp.), and anhydrous alcohol for approximately 15 min. The Nafion content in the dry catalyst layer was 33 wt%. The suspension was pipetted onto the gas diffusion layer and finally heated at 80ºC for 3 hours. The weight difference was measured and used to calculate the loading of the catalysts. A suspension consisting of 40 wt % Pt/C catalysts (Johnson-Matthey In. UK), 5 wt % Nafion solution (DuPont) (25wt% in the catalyst layer), and anhydrous alcohol was used to prepare the anode. The Pt loading was controlled at 0.3 mg cm^{-2} on the anodic side. The MEA was prepared by hot-pressing the cathode, Nafion 112 membrane (DuPont, 50 μm), and the anode at 137ºC and 5 MPa for 2 min. The Nafion 112 membrane (DuPont) was pretreated with 3 vol. % H_2O_2 and 0.5 M H_2SO_4 for 1 h to remove impurities. The membrane was then washed several times with hot ultrapure water. Pure hydrogen and oxygen were supplied to the anode and cathode at a flow rate of 150 and 200 mL min^{-1}, respectively.

Electrical resistances measurements

The electrical measurement method adopted here was previously reported. [1] In briefly, the electrical resistances were determined by using a homemade button cell with an active surface area of 0.95 cm^2 (see the simple illustration in Figure S9). The sample is inserted between two smooth polished steel discs. A

Solartron SI 1287 electrochemical interface equipped with a Solartron SI 1260 impedance/gain-phase analyzer coupling system was used. The operating frequency range was between 10 mHz and 100 kHz, the DC potential was 0 V compared to an open circuit, and the AC amplitude was 10 mV. In this case, the phase angle between the voltage applied and the current induced is zero; the impedance of the sample as a function of frequency is present as a horizontal line. The value of resistance of sample is equal to the impedance; and the |Z| -axis in the Bode directly show the resistance. The cell area is 0.95 cm^{-2}.

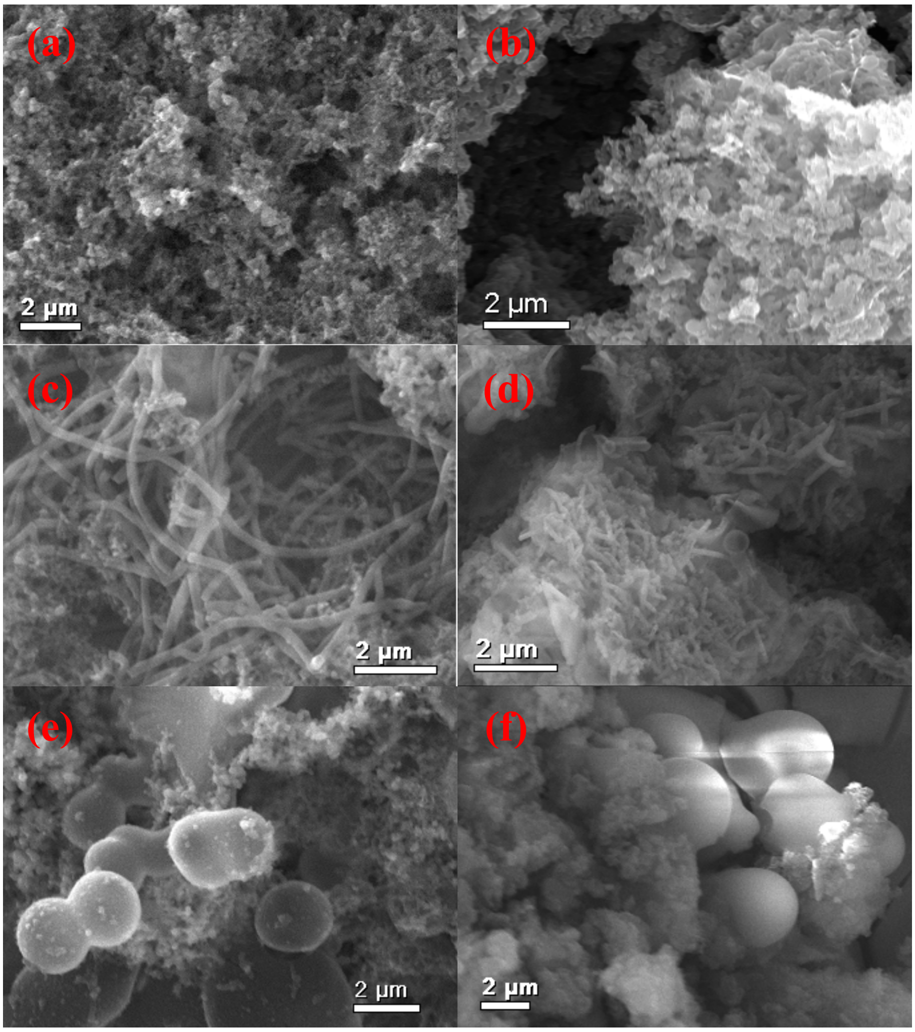

Figure S1. SEM images of as-prepared 3D PANI network (a), PANI nanotubes (c), PANI nanoshell (e), and their corresponding carbonized products: CPANI-3D-Fe-NaCl (b), CPANI-NT-Fe-NaCl (d), and CPANI-NS-Fe-NaCl (f).

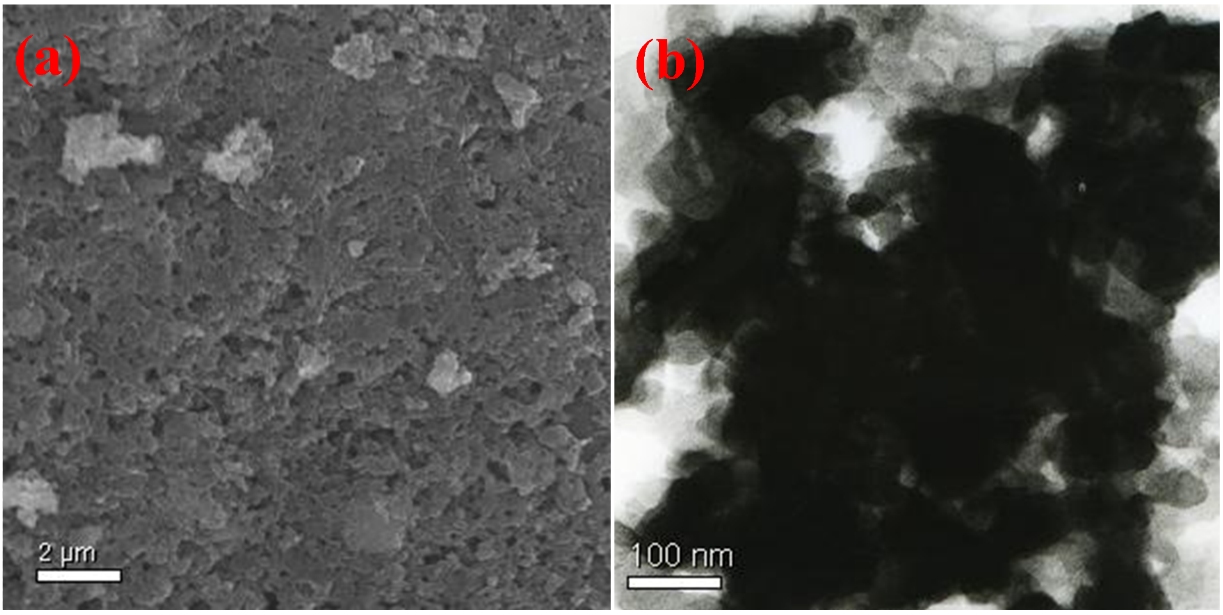

Figure S2.SEM image (a) and TEM image (b) of CPANI.

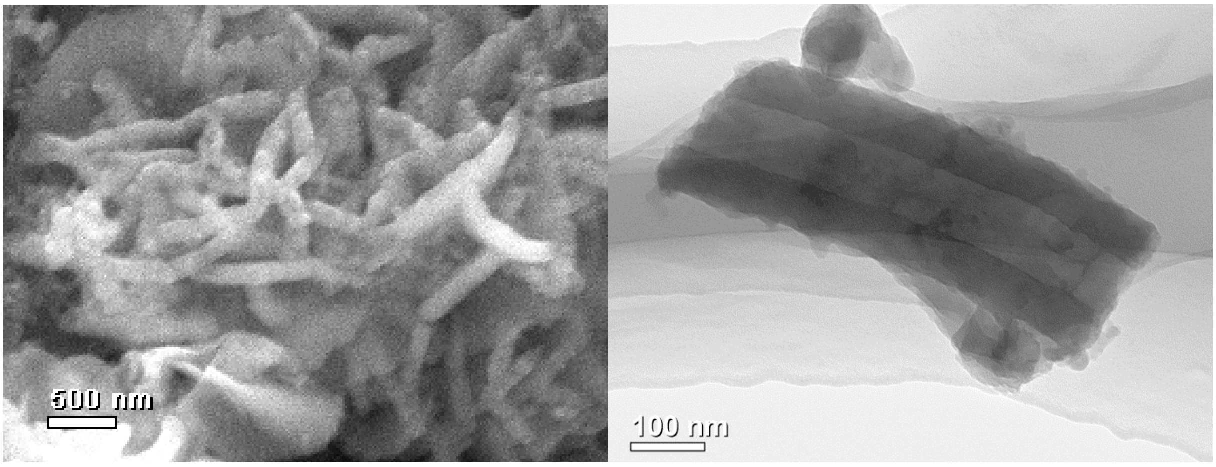

Figure S3.SEM image (a) and TEM image (b) of CPANI-NT-Fe-NaCl.

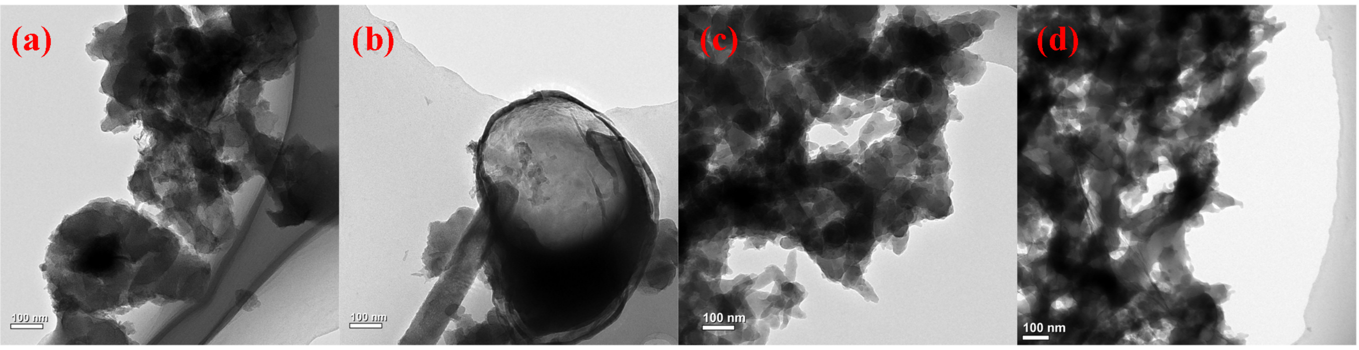

Figure S4.TEM image (a) (b) of CPANI-Fe, CPANI-NaCl (c) and CPANI-Fe-NaCl (d).

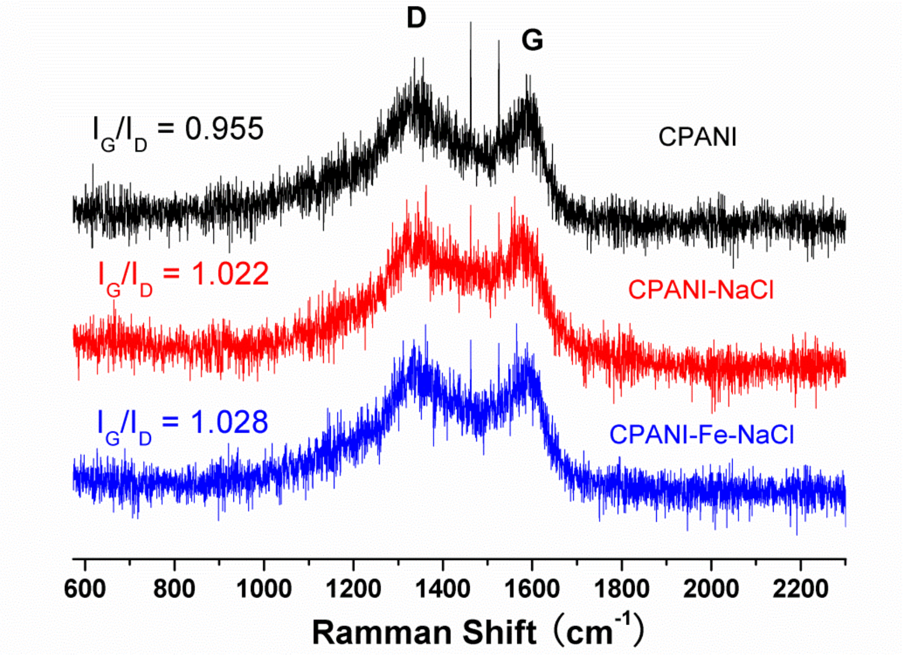

Figure S5. Raman spectra of CPANI-Fe-NaCl (blue), CPANI-NaCl (red) and CPANI (black).

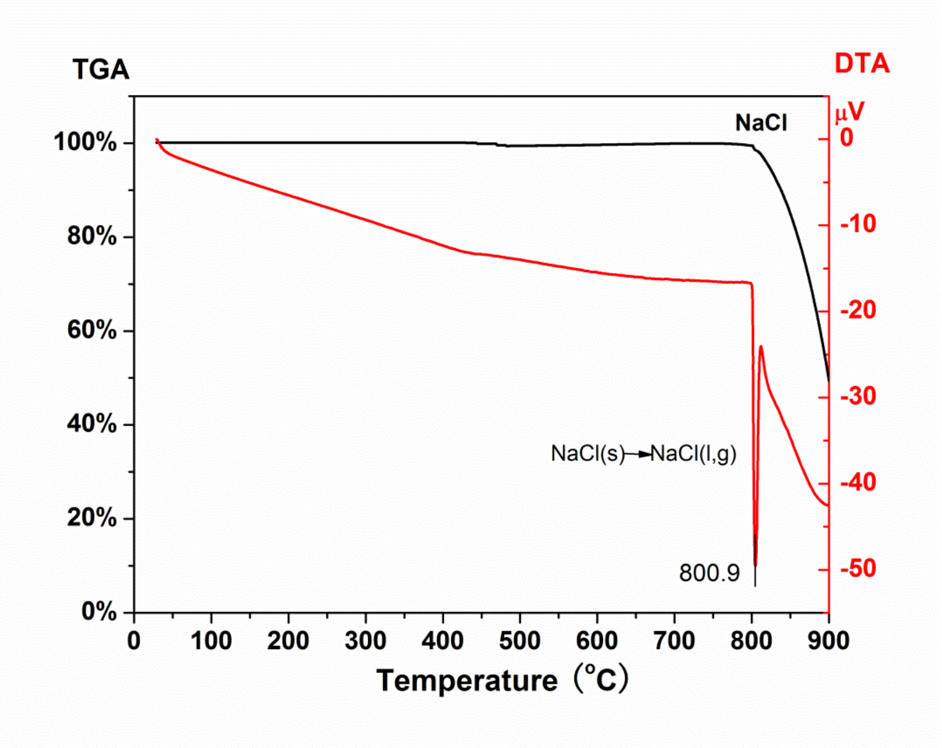

Figure S6. TGA-DTA plot of NaCl.

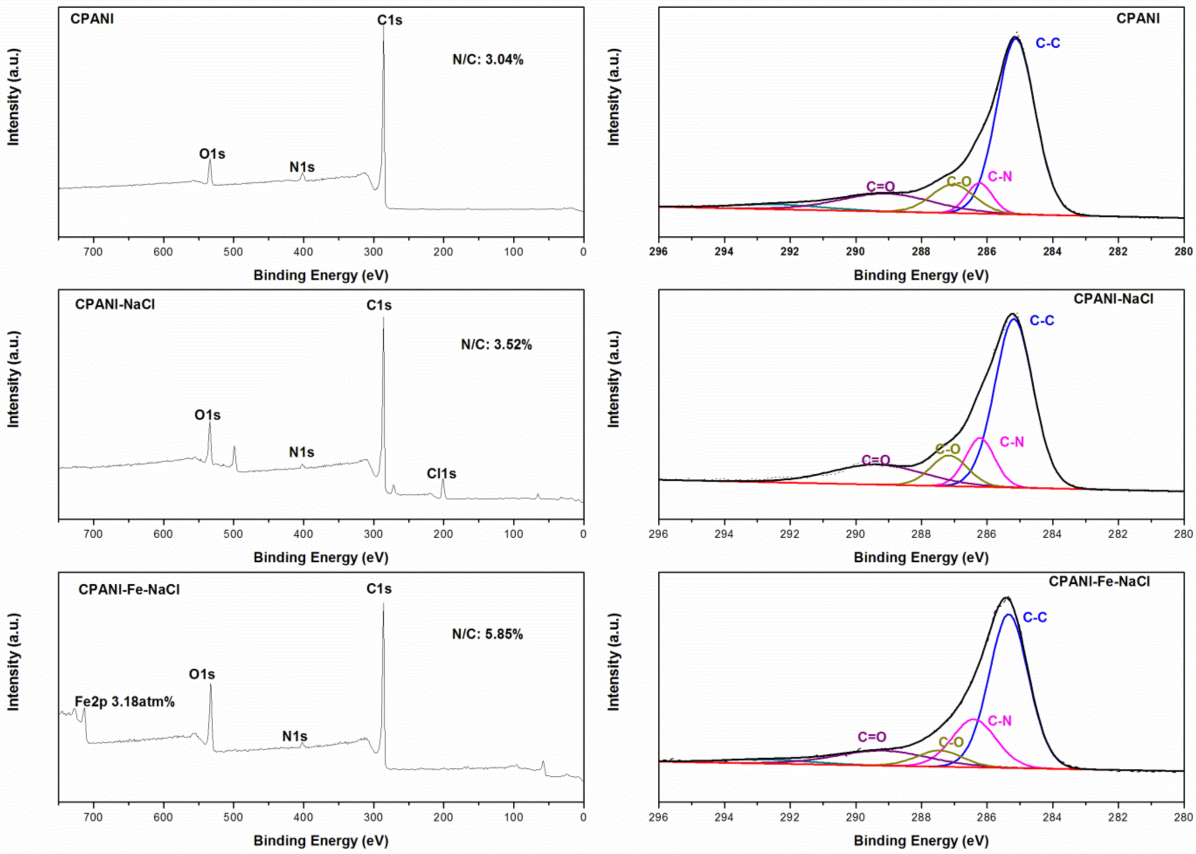

Figure S7. XPS spectra of CPANI, CPANI-NaCl and CPANI-Fe-NaCl. Corresponding O1s XPS spectra.

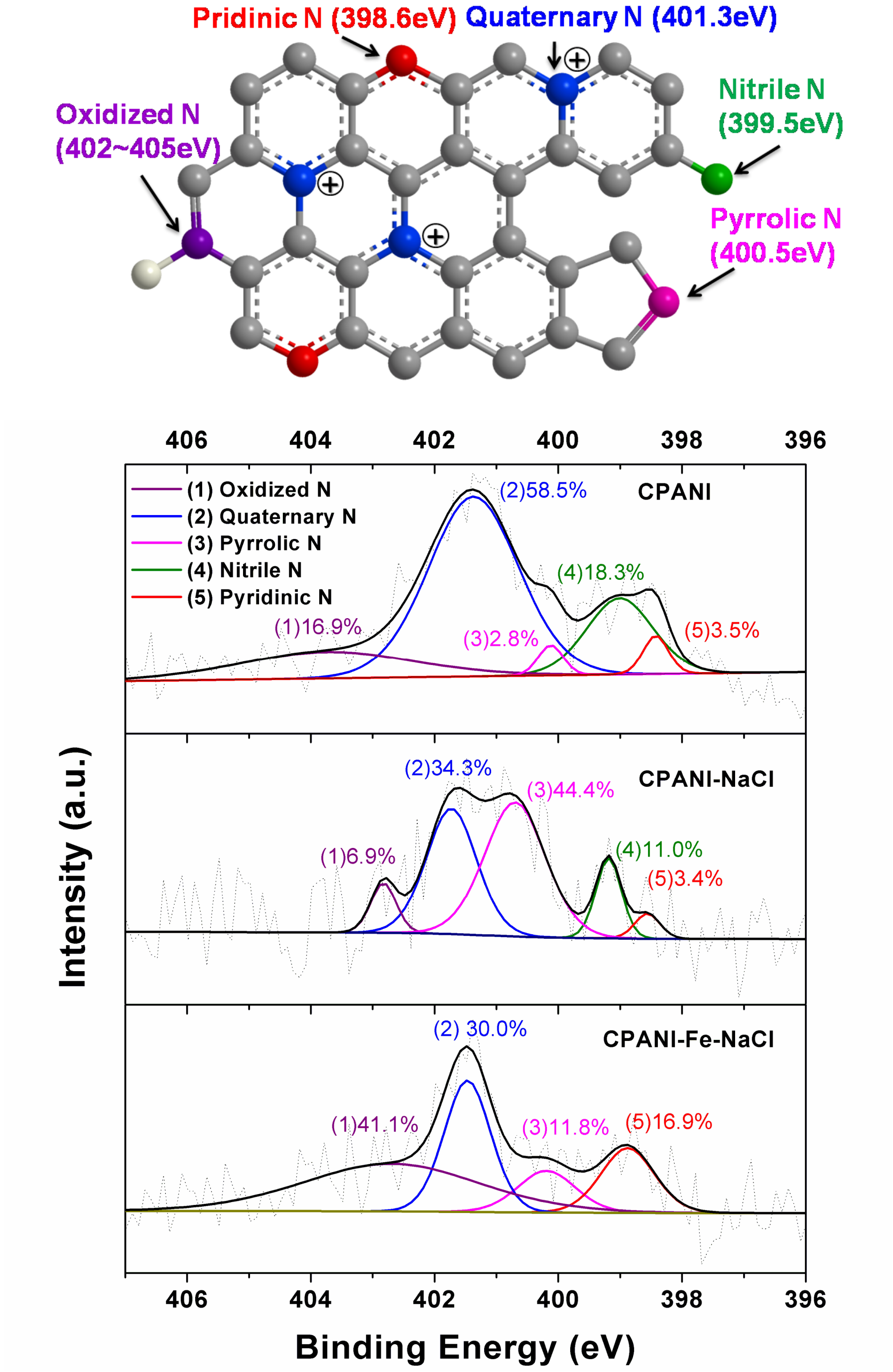

Figure S8. XPS spectra of N 1 s in CPANI, CPANI-NaCl, and CPANI-Fe-NaCl.

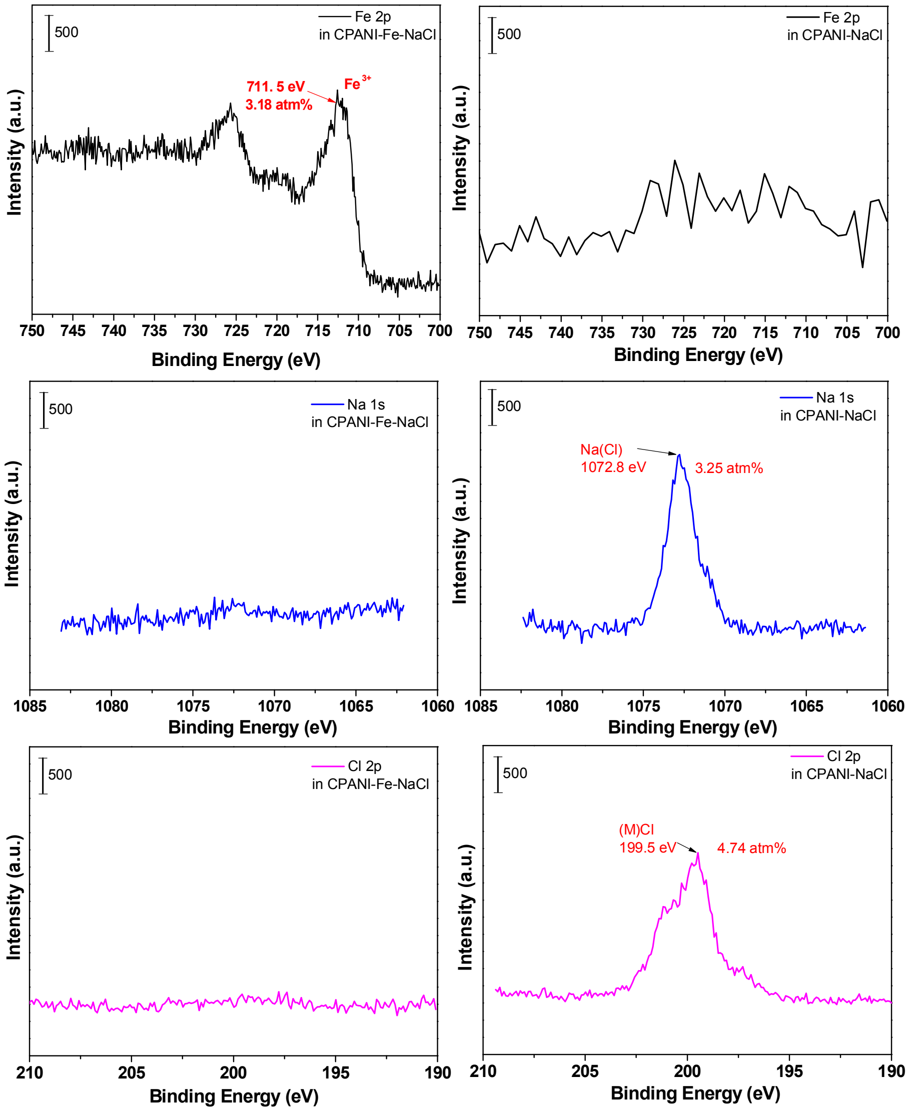

Figure S9. XPS spectra of Fe 2 p, Na 1 s, and Cl 2p in CPANI-NaCl, and CPANI-Fe-NaCl.

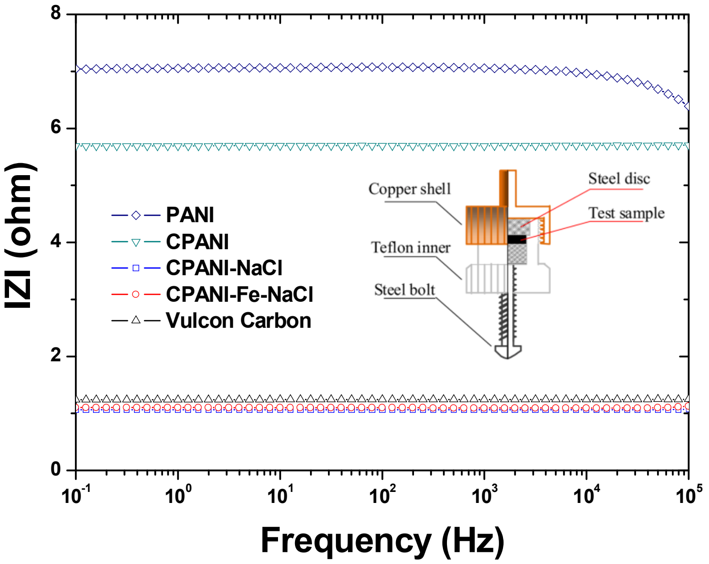

Figure S10. Bode spectra obtained through the application of a sinewave with an amplitude of 5.0 mV from 10 mHz to 100 kHz for differentcatalysts.

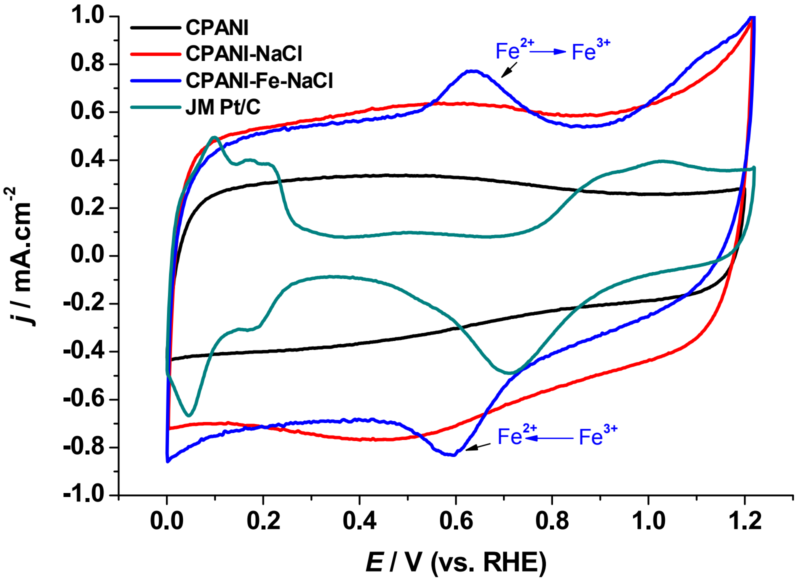

Figure S11. CVs of JM Pt/C-, CPANI-, CPANI-Fe-NaCl, and CPANI-NaCl-modified GC electrodes in an N_2-saturated 0.5 M H_2SO_4 solution. The catalyst loading was 0.6 mg cm^{-2}. The loading is 50 μgPtcm^{-2} for Pt/C (40%).

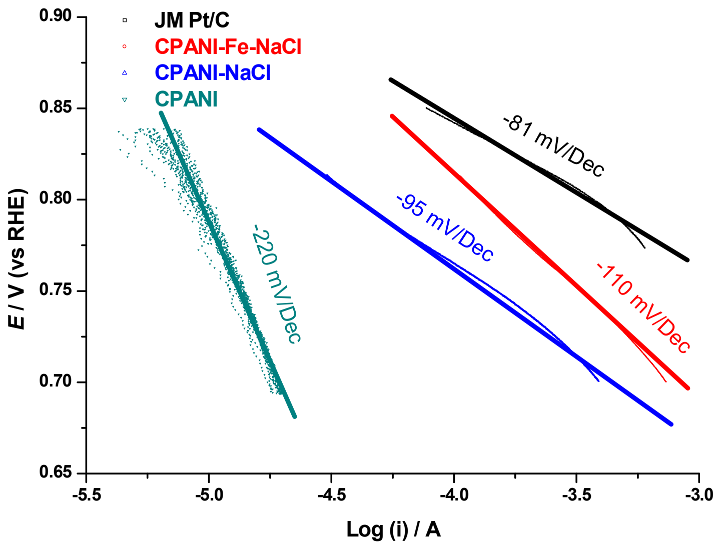

Figure S12. Tafel slops of the electrodes assembly fabricated with the JM Pt/C, CPANI, CPANI-Fe-NaCl and CPANI-Fe catalysts in 0.1 m $HClO_4$, scan rate 10mV s^{-1}.

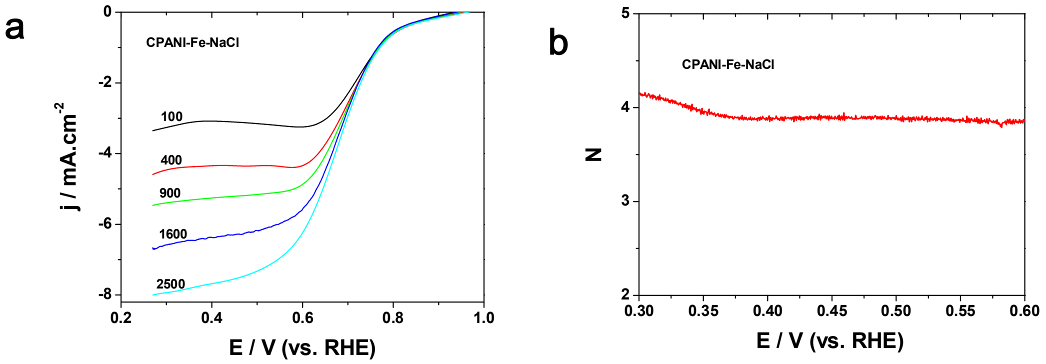

Figure S13. (a) RDE test of CPANI-Fe-NaCl -coated GC in an O_2-saturated 0.5 M H_2SO_4 solution at a scan rate of 10 mVs^{-1}.The catalyst loading was 0.6 mg cm^{-2}. (b) The number of transfer electron for ORR on the CPANI-Fe-NaCl -coated GC calculated by K-L plot on the basis of RDE test.

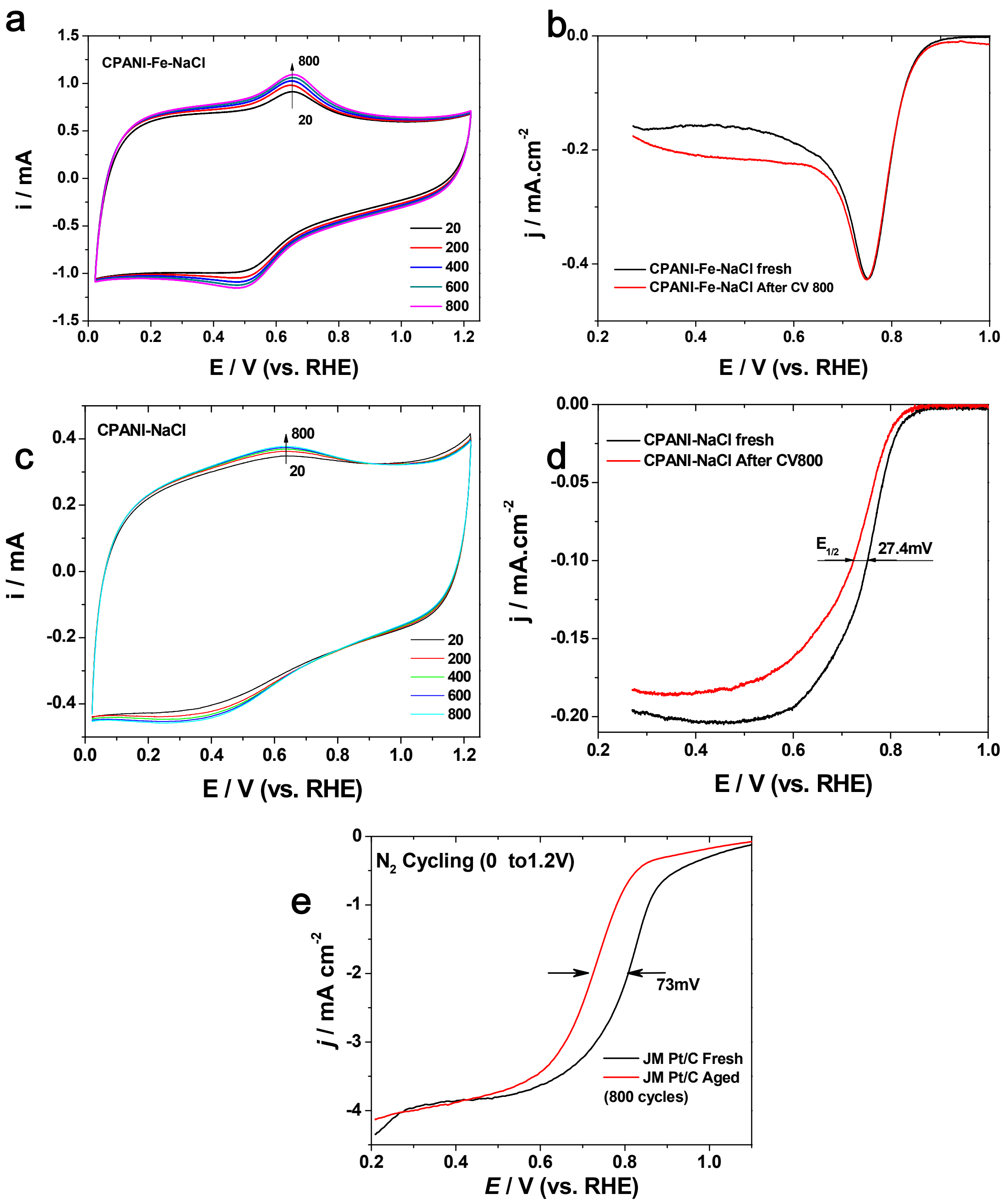

Figure S14. CVs of (a) CPANI-Fe-NaCl- and (c) CPANI-NaCl-modified GC electrodes in an N_2-saturated 0.5 M H_2SO_4 solution. LSV of (b) CPANI-Fe-NaCl, (d) CPANI-NaCl (40%) and (e) JM Pt/C-modified GC electrodes in an O_2-saturated 0.5 M H_2SO_4 solution before and after N_2 cycling stability tests at a scan rate of 10 mVs^{-1}. The loading is 25 μgPtcm^{-2} for Pt/C (40%) and is 0.6 mg cm^{-2} for non-Pt catalyst.

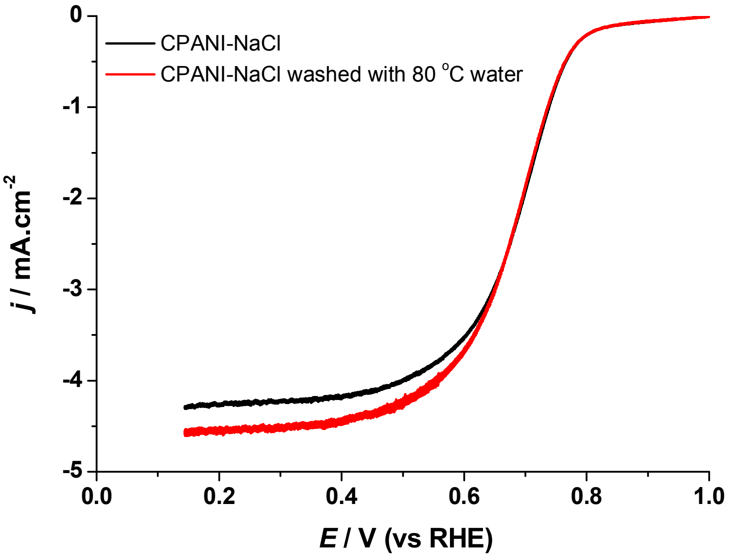

Figure S15. Steady-state plots of ORR polarization for CPANI-NaCl catalysts in O_2-saturated 0.5 m H_2SO_4.

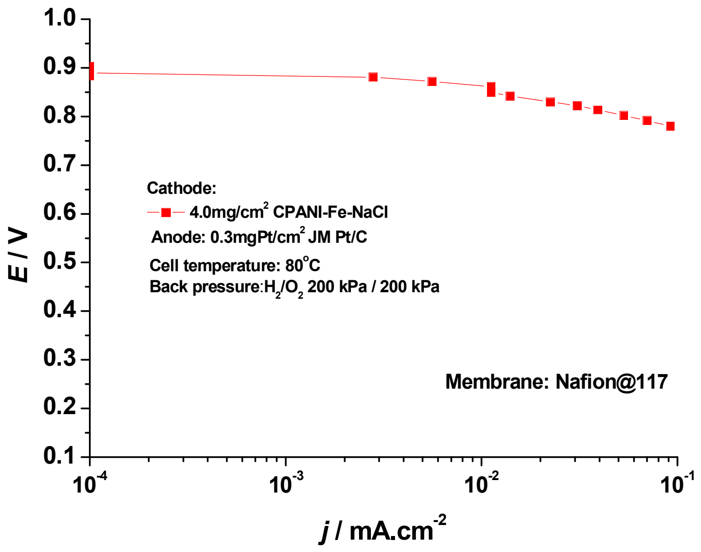

Figure S16. Polarization curves of membrane electrode assemblies fabricated with the CPANI-Fe-NaCl cathode catalysts, the Nafion 117 membrane (DuPont) with a thickness of 183 μm was used to avoid some electrical shortage in the membrane.

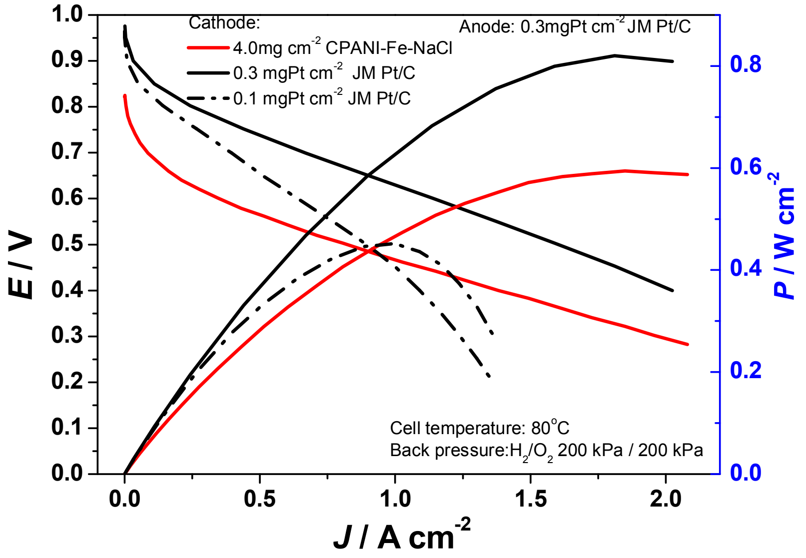

Figure S17. Polarization curves of membrane electrode assemblies fabricated with the CPANI-Fe-NaCl and JM Pt/C cathode catalysts, the Nafion 112 membrane (DuPont).

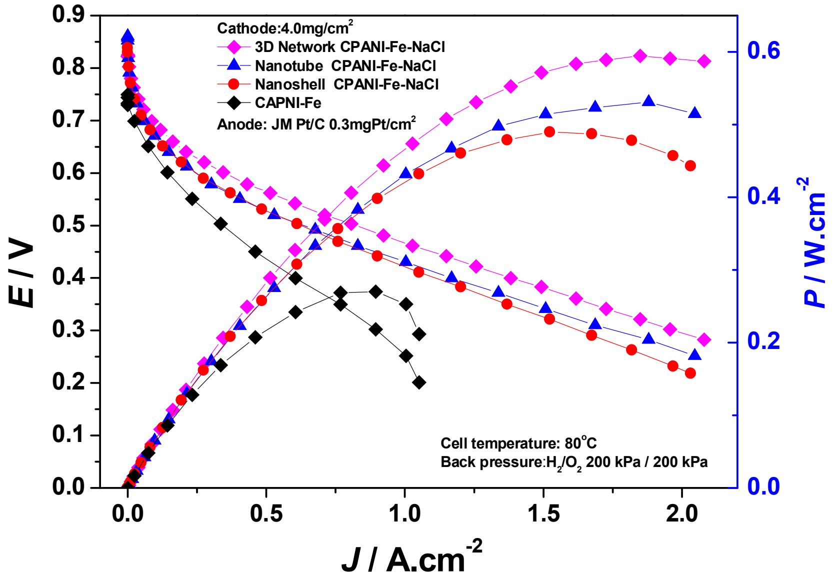

Figure S18. Polarization curves of membrane electrode assemblies fabricated with the CPANI-Fe-NaCl and CPANI-Fe cathode catalysts, the Nafion 112 membrane (DuPont).

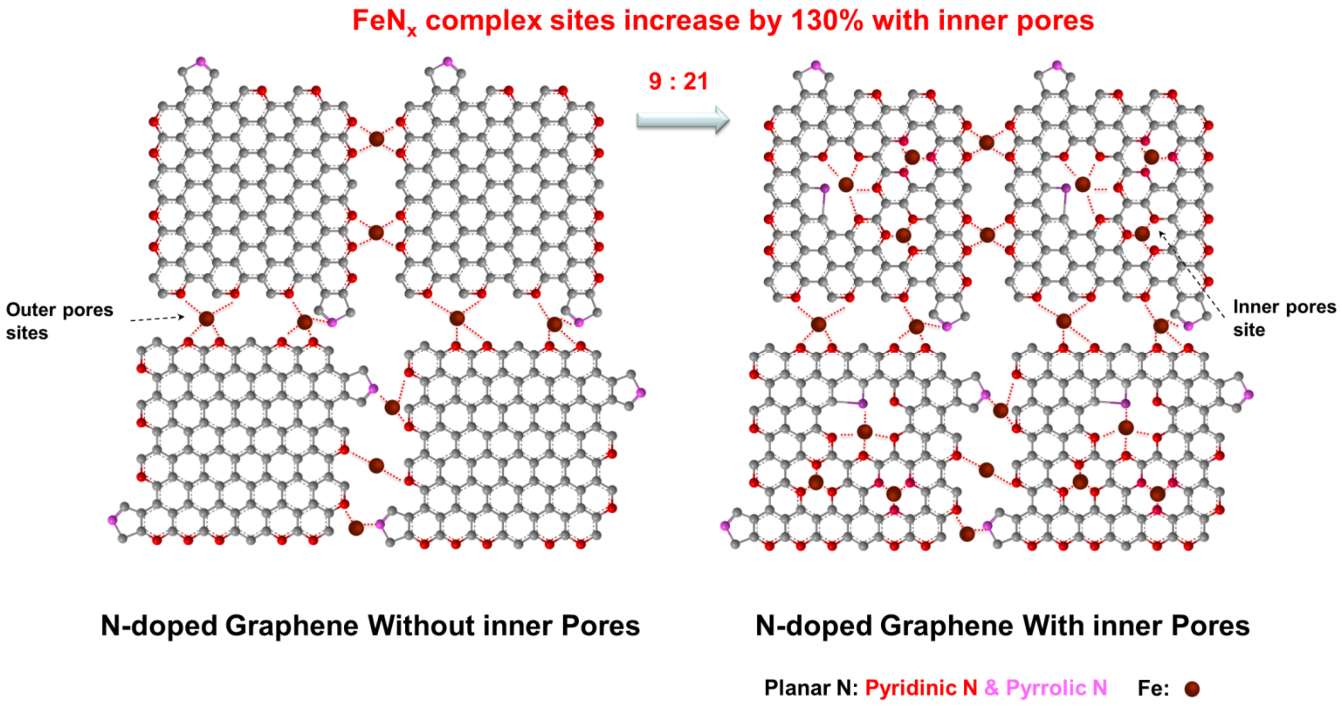

Figure S19. Schematic of the increase of the FeNx complex active sites with inner pores.

Reference

[1] Ding, W.; Wei, Z.-D.; Chen, S. G.; Qi, X. Q.; Yang, T.; Hu, J. -S.; Wang, D.; Wan, L. -J.; Alvi, S. F.; Li, L. *Angew. Chem. Int. Ed.* **2013**, 52, 11755 –11759